1404 *Biochemistry* **2010,** *49,* 1404–1417
DOI: 10.1021/bi902132u

BIOCHEMISTRY
including biophysical chemistry & molecular biology
Article

Inactivation of *Lactobacillus leichmannii* Ribonucleotide Reductase by 2′,2′-Difluoro-2′-deoxycytidine 5′-Triphosphate: Covalent Modification[†]

Gregory J. S. Lohman[‡] and JoAnne Stubbe*[,‡,§]

[‡]*Department of Chemistry and* [§]*Department of Biology, Massachusetts Institute of Technology, Cambridge, Massachusetts 02139*

Received December 11, 2009; Revised Manuscript Received January 18, 2010

ABSTRACT: Ribonucleotide reductase (RNR) from *Lactobacillus leichmannii*, a 76 kDa monomer using adenosylcobalamin (AdoCbl) as a cofactor, catalyzes the conversion of nucleoside triphosphates to deoxynucleotides and is rapidly (< 30 s) inactivated by 1 equiv of 2′,2′-difluoro-2′-deoxycytidine 5′-triphosphate (F_2CTP). [1′-^{3}H]- and [5-^{3}H]F_2CTP were synthesized and used independently to inactivate RNR. Sephadex G-50 chromatography of the inactivation mixture revealed that 0.47 equiv of a sugar was covalently bound to RNR and that 0.71 equiv of cytosine was released. Alternatively, analysis of the inactivated RNR by SDS−PAGE without boiling resulted in 33% of RNR migrating as a 110 kDa protein. Inactivation of RNR with a mixture of [1′-^{3}H]F_2CTP and [1′-^{2}H]F_2CTP followed by reduction with $NaBH_4$, alkylation with iodoacetamide, trypsin digestion, and HPLC separation of the resulting peptides allowed isolation and identification by MALDI-TOF mass spectrometry (MS) of a ^{3}H/^{2}H-labeled peptide containing C_{731} and C_{736} from the C-terminus of RNR accounting for 10% of the labeled protein. The MS analysis also revealed that the two cysteines were cross-linked to a furanone species derived from the sugar of F_2CTP. Incubation of [1′-^{3}H]F_2CTP with C119S-RNR resulted in 0.3 equiv of sugar being covalently bound to the protein, and incubation with $NaBH_4$ subsequent to inactivation resulted in trapping of 2′-fluoro-2′-deoxycytidine. These studies and the ones in the preceding paper (DOI: 10.1021/bi9021318) allow proposal of a mechanism of inactivation of RNR by F_2CTP involving multiple reaction pathways. The proposed mechanisms share many common features with F_2CDP inactivation of the class I RNRs.

The nucleoside 2-deoxy-2′,2′-difluorocytidine (F_2C[1] or Gemzar) is a clinically used anticancer drug that targets ribonucleotide reductase (RNR) and DNA polymerase in addition to several other proteins involved in nucleotide metabolism (*1*−*3*). Studies have shown that F_2C is therapeutically effective against a range of cancers (*4*−*17*) with tolerable levels of toxicity. The mechanism by which F_2C inactivates RNRs has been the subject of a number of investigations (*18*−*21*), modeled on our detailed understanding of the mechanism by which 2′-substituted 2′-deoxynucleotides inhibit these enzymes (Scheme 1) (*22*). These studies revealed that gemcitabine 5′-diphosphate (F_2CDP) in the case of the class I RNRs (*Escherichia coli* and humans forms are both diphosphate reductases, RDPR) and gemcitabine 5-triphosphate (F_2CTP) in the case of the class II RNR from *Lactobacillus leichmannii* (a nucleoside triphosphate reductase, RTPR) are potent, mechanism-based inhibitors (*20*, *21*, *23*−*25*).

Since the discovery of Thelander and Eckstein that 2′-chloro-2′-deoxynucleotides and 2′-azido-2′-deoxynucleotides are inhibitors of RNRs, a large number of studies have led to the general mechanism of inhibition shown in Scheme 1 (X = Cl^-, F^-, or N_3^-). In this mechanism, a protein thiyl radical initiates the reduction process by abstraction a 3′-hydrogen atom from the nucleotide, which is followed by rapid loss of the 2′-substituent. The glutamate residue in the RNR active site likely facilitates this process by deprotonation of the 3′-hydroxyl, and a cysteine facilitates C−X bond cleavage by protonation, depending on X (OH, Cl^-, F^-, or N_3^-). The 3′-ketone with an adjacent 2′-radical (**3**, Scheme 1) is produced in all cases. This intermediate then experiences different fates depending on the conformation on the nucleotide in the active site, the charge on the leaving group, and the protonation state of the protein residues. In some cases, **3** is reduced from the top face (β face of the nucleotide) and in others from the bottom face (α face). The 3′-ketodeoxynucleotide **4** is generated in both pathways. Recent computational studies have suggested that when X is anionic, the hydrogen bond network on the α face of the nucleotide is distinct from the hydrogen bonding when neutral water is released (*26*). The binding affinity of **4** for the enzyme was calculated to be substantially reduced with X^- released relative to H_2O. Furthermore, when X^- was F^-, the calculations suggested that it was released prior to dissociation of **4**. When **4** dissociates from the active site, our previous studies showed that it decomposes in solution to generate free nucleic acid base, pyrophosphate (tripolyphosphate), and a reactive furanone (**5**). In the case of top face reduction (pathway A), alkylation is responsible for inactivation. In the case of β face reduction (pathway B), alkylation and destruction of the radical initiator are responsible for inactivation.

[†]Funding for this study was provided in part by National Institutes of Health Grant GM-29595.

*To whom correspondence should be addressed. Telephone: (617) 253-1814. Fax: (617) 258-7247. E-mail: stubbe@mit.edu.

[1]Abbreviations: RNR, ribonucleotide reductase; Gemzar or F_2C, 2′,2′-fluoro-2′-deoxycytidine; F_2CDP, 2′,2′-difluoro-2′-deoxycytidine 5′-diphosphate; F_2CTP, 2′,2′-difluoro-2′-deoxycytidine 5′-triphosphate; RTPR, ribonucleoside triphosphate reductase; AdoCbl, adenosylcobalamin; SF, stopped flow; RFQ, rapid freeze quench; SA, specific activity; dCK, deoxycytidine kinase; TR, thioredoxin; TRR, thioredoxin reductase; TEAB, triethylammonium bicarbonate; PEP, phosphoenolpyruvate; SEC, size exclusion chromatography; PSD, post-source decay; HMDS, hexamethyldisilazide; α, RNR large subunit; β, RNR small subunit.

 Published on Web 01/20/2010

Scheme 1: Proposed Mechanism of Inactivation of RNR by 2′-Substituted Mechanism-Based Inhibitors

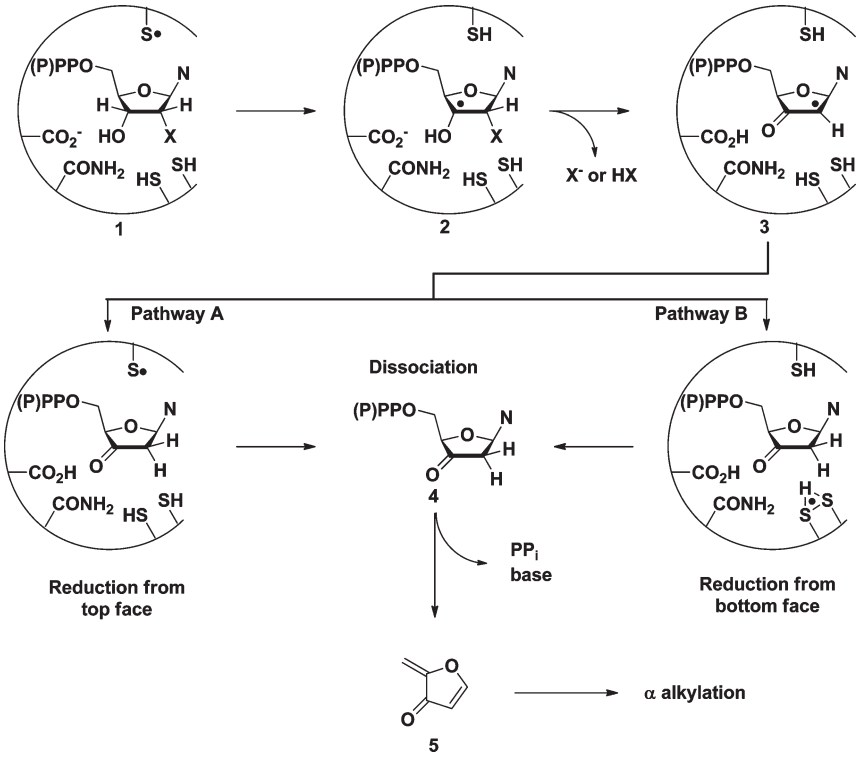

Studies with gemcitabine differ from those with other 2′-substituted mechanism-based inhibitors in that there are two substituents at C-2′. In fact, our initial studies of RNRs from *E. coli* and *L. leichmannii* suggested that the mechanism differed from the paradigm in Scheme 1 (*20*, *21*). In the case of RTPR, its incubation with 1 equiv of F_2CTP resulted in a 90% loss of catalytic activity within 30 s. Analysis of products after 30 min revealed that that the inactivation was accompanied by release of both fluorides, formation of 0.84 equiv of 5′-deoxyadenosine from the adensoylcobalamin (AdoCbl) cofactor, and ultimately covalent attachment of cobalamin to C_{419}, one of the cysteines located on the α face of the nucleotide involved in supplying the reducing equivalents for the reduction. In addition, kinetic studies by stopped flow (SF) spectroscopy revealed that cob(II)alamin was generated with a k_{obs} of 50 s^{-1} when 1 equiv of F_2CTP was reacted with RTPR, suggesting that the rate constant would be similar to that of cob(II)alamin formation with CTP (250 s^{-1}), if the nucleotide was present at saturating levels. Rapid freeze quench (RFQ) EPR experiments showed initial formation of the same exchange-coupled thiyl radical−cob(II)alamin species (22 ms) observed with CTP, followed by stoichiometric conversion to a new radical−cob(II)alamin species over 255 ms, suggesting thiyl radical-mediated nucleotide radical formation. Efforts to further study the mechanism of this inactivation were hampered by the unavailability of the isotopically labeled gemcitabine analogues.

We now report synthesis of 1′-^{2}H-, 1′-^{3}H-, and 5-^{3}H-labeled gemcitabine nucleotides by a combination of chemical and enzymatic methods. Using these probes, we now report, in this paper and the preceding paper (DOI: 10.1021/bi9021318), on the mechanism by which F_2CTP inhibits the class II *L. leichmannii* RTPR (*27*). We demonstrate that 0.47 equiv of sugar from F_2CTP covalently labels RTPR and that in contrast to our previous studies, cytosine (~0.7 equiv) is released to solution. Use of a mixture of [1′-^{2}H,^{3}H]F_2CTP for the inactivation of RTPR was critical for identification by mass spectrometric methods, the peptides modified by a sugar moiety derived from F_2CTP. In the preceding paper (DOI: 10.1021/bi9021318), [1′-^{2}H]F_2CTP has been used to establish that the new radical generated by the thiyl radical−cob(II)alamin species is nucleotide-derived (*27*). We also describe the fate of the adenosylcobalamin and the structure of an unusual nucleotide trapped with $NaBH_4$ which we believe is derived from the observed nucleotide radical intermediate. These studies together have allowed us to formulate mechanisms for RTPR inactivation that, while complex, do follow the paradigms shown in Scheme 1.

MATERIALS AND METHODS

2-Deoxy-3,5-di-*O*-benzoyl-2,2-difluororibonolactone was a gift of Eli Lilly & Co. All reagents were purchased from Sigma or Mallinckrodt and used without further purification unless otherwise indicated. Analytical TLC was performed on an E. Merck silica gel 60 F254 plate (≤0.25 mm). Compounds were visualized by cerium sulfate-ammonium molybdate stain and heating or by exposure to UV light. Human deoxycytidine kinase (dCK) expression plasmids were a gift from S. Eriksson (*28*), and the protein [specific activity (SA) of 150 nmol mg^{-1} min^{-1}] was expressed, purified, and stored in 20 mM Tris (pH 7.9), 0.5 M NaCl, 10 mM DTT, and 20% glycerol. UMP/CMP kinase expression plasmids were a kind gift from A. Karlsson (*29*). The protein was expressed and purified (SA of 2.1−4.8 μmol mg^{-1} min^{-1}) as described previously (*30*) and stored in 50 mM Tris (pH 8.0) and 10 mM reduced glutathione. Its concentration was determined by a Bradford assay with a BSA standard. Inorganic pyrophosphatase (baker's yeast) (SA of 868 units/mg) was obtained from Sigma as a lyophilized powder and taken up in 165 mM Tris (pH 7.2) immediately prior to use. Pyruvate kinase (rabbit muscle) (SA of 450 units/mg) was obtained from Sigma as a lyophilized powder and prepared as a 1200 units/mL

stock in 50 mM Tris (pH 7.5), 80 mM KCl, and 20 mM $MgCl_2$. Calf intestine alkaline phosphatase was purchased from Roche as a 20 units/μL stock in 100 mM Tris (pH 8.5). *E. coli* thioredoxin (TR, SA of 40 units/mg) and *E. coli* thioredoxin reductase (TRR, SA of 1320 units/mg) were isolated as previously described (*31*, *32*). RTPR (SA of 0.38−0.42 μmol mg^{-1} min^{-1}) was isolated as previously described (*33*), omitting the second anion exchange column. AdoCbl was handled with minimal exposure to light. All reaction mixtures including AdoCbl were kept wrapped in foil at all times. Transfer of AdoCbl-containing solutions was performed under dim or red light conditions. The following extinction coefficients were used: λ_{280} = 56755 at pH 7.0 for dCK, λ_{268} = 9360 at pH 7.0 for F_2C (*34*), λ_{271} = 9100 at pH 7.0 for cytidine, λ_{267} = 6100 at pH 7.0 for cytosine, and λ_{259} = 15400 at pH 7.0 for adenosine (*35*). UV−vis spectra were recorded on a Cary-3 spectrometer. Anion exchange column fractions were assayed using an Ultramark Bio-RAD fixed wavelength plate reader. Scintillation counting was performed using Emulsifier-Safe liquid scintillation counting cocktail (Perkin-Elmer) on a Beckman LS6500 multipurpose scintillation counter.

Synthesis of [*1′-*^{3}*H*]*-2-Deoxy-3,5-di-O-benzoyl-2,2-difluoro-1-O-methanesulfonyl-*D*-ribofuranoside* (***8****, Scheme S1 of the Supporting Information*) *(36, 37) and* [*1′-*^{3}*H*]*-*F_2C. F_2C was synthesized from 2-deoxy-3,5-di-*O*-benzoyl-2,2-difluororibonolactone (**6**) or the unblocked lactone by modifications of published procedures, and the reaction is summarized in Scheme S1 of the Supporting Information (*34*). Only the step to incorporate the tritium label at C-1′ is described in detail. All solid reagents were dried over P_2O_5 under vacuum overnight. All solvents and liquid reagents were distilled from CaH immediately before use, except mesyl chloride, which was distilled from P_2O_5. NaB^3H_4 (500 mCi of NaB^3H_4, SA of 14.22 Ci/mM, Perkin-Elmer) was combined with 152 mg or 4 mmol of $NaBH_4$ and the mixture dissolved in diglyme (4 mL) under N_2 to make a 1.0 M solution. A three-neck flask fitted with a coldfinger, gas inlet, and dropping funnel was assembled and connected to a 10 mL conical flask through an exit from the coldfinger using tygon tubing and a needle. This apparatus allowed B_2H_6 generated in the three-neck flask to be transferred to the 10 mL flask. The entire apparatus was flame-dried and cooled under N_2. The coldfinger attached to the three-neck flask was filled with dry ice and acetone. The NaB^3H_4 solution was added to the dropping funnel, and boron trifluoride diethyl etherate (1.25 mL, 10 mmol, 2.5 equiv) was added to the three-neck flask in an oil bath at room temperature. The conical flask was immersed in a dry ice/acetone bath and tetrahydrofuran (THF, 2 mL) added. The needle was immersed in the THF and the N_2 flow turned to a minimum. The borohydride solution was added dropwise over 1 h. The evolution of gas was immediately evident, and a white precipitate ($NaBF_4$) (*38*) formed over the course of the reaction. The oil bath was heated to 70 °C for 30 min to distill off any remaining B_2H_6. The apparatus was disassembled, leaving the conical flask under N_2 in the dry ice/acetone bath. The concentrations of BH_3 and THF were established by titration (*36*, *37*). The BH_3/THF solution was transferred to an ice/salt bath (−15 °C), and 2-methyl-2-butene (1.03 mL, 9.6 mmol) was added slowly, dropwise via syringe over 1 h. The reaction mixture was stirred for an additional 1 h at −15 °C. The solution of disiamylborane was transferred to an ice bath (0 °C), and a solution of **6** (188 mg, 0.5 mmol) in 1 mL of THF was added dropwise via syringe over 30 min. The reaction mixture was stirred for 1 h at 0 °C followed by 16 h at room temperature. Water (1 mL) was then added slowly. Foaming occurred as H_2 gas evolved. The flask was equipped with a reflux condenser, and the mixture was refluxed for 30 min and then cooled to 0 °C and the reflux condenser removed. Hydrogen peroxide (1 mL, 30% solution) was added dropwise over 5 min, along with enough 2 N NaOH to keep the pH at 7.5−8.0 (monitored with a microelectrode, ~200 mL over the course of the quench). The mixture was poured into EtOAc (100 mL) and washed with water (2 × 50 mL). The organic layer was dried over $MgSO_4$ and filtered and the solvent removed in vacuo.

Residue **7** (Scheme S1 of the Supporting Information) was dried over P_2O_5 and dissolved in CH_2Cl_2 (5 mL). The reaction mixture was cooled to 0 °C, and triethylamine (TEA, 0.5 mL, distilled from KOH) and mesyl chloride (0.39 mL, 5 mmol) were added. The ice bath was removed and the reaction mixture stirred for 3 h at room temperature. The reaction mixture was diluted to 100 mL with CH_2Cl_2 and the organic layer washed with 1 N HCl, water, saturated $NaHCO_3$, and water. The organic layer was dried over $MgSO_4$ and filtered and the solvent removed in vacuo. Purification using silica gel chromatography (1 cm × 15 cm column, 4:1 hexane/ethyl acetate elutant) yielded **8** (143 mg, 0.313 mmol, 63%) as a clear oil. The ^{1}H NMR spectrum was consistent with previously reported data (*34*).

Bis(trimethylsilyl)cytosine (**9**) was made from cytosine (*39*) and coupled to **8** using trimethylsilyl trifluoromethanesulfonate as previously described (*34*). Compound **10** as a 6:4 α/β mixture was obtained and quantified by UV absorbance (ε_{268} = 9360 at pH 7.0) to give 190.5 mmol (76% from **8**). ^{1}H NMR was consistent with that reported for **10** (*34*), and it was judged to be >95% pure.

2′-Deoxy-2′,2′-difluorocytidine 5′-Monophosphate (*F_2CMP*) *(28, 30)*. F_2C was converted to its monophosphate directly from the α/β mixture. The reaction mixture contained, in a final volume of 1 mL, 5 mM β-F_2C, 10 mM ATP, 2 mM DTT, 0.5 mg/mL BSA, 1.4 mg/mL human dCK, 50 mM Tris (pH 7.6), 100 mM KCl, and 10 mM $MgCl_2$. The reaction was initiated by addition of dCK and the mixture incubated at 37 °C for 45 min. The reaction mixture was loaded on a DEAE-Sephadex A-25 column (20 mL, 20 cm × 1 cm) equilibrated in 5 mM triethylammonium bicarbonate (TEAB) (pH 6.8) and the column washed with 50 mL of 5 mM TEAB. The product was eluted using a 100 mL × 100 mL linear gradient from 5 to 400 mM TEAB. Fractions (5 mL) were assayed for A_{260}; the nucleotide-containing fractions were combined, and the solvent was removed in vacuo. ^{1}H NMR analysis of the flow-through from the initial wash showed only the presence of the α anomer of **10** (*34*). F_2CMP eluted at 250 mM TEAB (4.45 mmol, 90%): ^{1}H NMR (500 MHz, D_2O, selected peaks) δ 7.83 (d, J = 7.5 Hz, 1H), 6.15 (t, J = 6.4 Hz, 1H), 6.05 (d, J = 7.5 Hz, 1H), 4.36 (dd, J = 12.4, 21.1 Hz, 1H), 4.02−4.09 (m, 2H), 3.91−3.96 (m, 1H); ^{31}P NMR (121.5 MHz, D_2O, phosphoric acid external reference) δ 4.6.

2′-Deoxy-2′,2′-difluorocytidine 5′-Diphosphate (*F_2CDP*) *(29, 30, 40)*. The reaction mixture contained, in a final volume of 5 mL, 2 mM F_2CMP, 8 mM ATP, 2 mM DTT, 50 mM Tris (pH 8), 25 mM $MgCl_2$, and 66.5 mg/mL UMP-CMP kinase. The reaction mixture was incubated for 30 min at 37 °C, diluted to 50 mL with cold water, and loaded onto a DEAE-Sephadex A-25 column (30 mL, 18 cm × 1.5 cm). The column was washed with water (100 mL) and the product eluted with a 400 mL × 400 mL linear gradient from 0 to 600 mM TEAB. The fractions (7.5 mL) were assayed by A_{260}, with F_2CDP eluting along with ADP at 450 mM TEAB. The fractions were combined, and the solvent

was removed in vacuo. The product was coevaporated with 50% ethanol in water (5 × 20 mL) to remove excess TEAB. To remove contaminating adenosine nucleotides, this material was dissolved in water (24 mL) and $NaIO_4$ (0.5 mmol, 1 mL of a 0.5 M solution) was added. The reaction mixture was incubated for 10 min at 37 °C, and then methylamine (2.5 mmol, 640 mL of a 3.9 M solution in water, pH adjusted to 7.5 with phosphoric acid) was added and the reaction mixture incubated for an additional 20 min. The reaction was quenched by addition of rhamnose (1 mmol, 1 mL of a 1 M solution). To this mixture was added 6.6 mL of 8 mM $MgCl_2$, 165 mM Tris (pH 7.2), and yeast inorganic pyrophosphatase [165 mL of a 50 units/mL stock in 165 mM Tris (pH 7.2)] to give final concentrations of 2 mM $MgCl_2$, 55 mM Tris (pH 7.2), and 0.25 units/mL inorganic pyrophosphatase. This mixture was incubated for 45 min at 37 °C, diluted to 300 mL with cold water, and loaded onto a DEAE-Sephadex A-25 column (30 mL, 18 cm × 1.5 cm). The column was washed with water (100 mL) and the product eluted with a 400 mL × 400 mL linear gradient from 0 to 600 mM TEAB. The fractions (7.5 mL) were assayed by A_{260}; the F_2CDP-containing fractions eluting at 450 mM TEAB were combined, and the solvent was removed in vacuo. The product was redissolved in water (1 mL) giving 5.6 mmol (56% yield): ^{1}H NMR (500 MHz, D_2O) δ 7.71 (d, J = 7.7 Hz, 1H), 6.09 (t, J = 7.2 Hz, 1H), 5.96 (d, J = 7.7 Hz, 1H), 4.40 (dd, J = 13.3, 22.2 Hz, 1H), 4.05−4.21 (m, 2H), 3.99−4.03 (m, 1H); ^{31}P NMR (121.5 MHz, D_2O, phosphoric acid external reference) δ −9.5 (d, J = 22.1 Hz), −10.6 (d, J = 22.1 Hz). The ^{31}P NMR showed no contamination with inorganic pyrophosphate.

2′-Deoxy-2′,2′-difluorocytidine 5′-Triphosphate (*F_2CTP*). The reaction mixture (20 mL) contained 2 mM F_2CDP, 4 mM phosphoenolpyruvate (PEP), 50 mM Tris (pH 7.5), 80 mM KCl, 20 mM $MgCl_2$, and 120 units/mL pyruvate kinase. The reaction mixture was incubated at 37 °C for 1 h. The mixture was then diluted with cold water (50 mL) and loaded on a DEAE-Sephadex A-25 column (60 mL, 20 cm × 2 cm), and the column was washed with water (100 mL) and the product eluted with a 400 mL × 400 mL linear gradient from 0 to 750 mM TEAB. The fractions (10 mL) were assayed for A_{260}. The triphosphate-containing fractions eluting at 550 mM TEAB were combined, and the solvent was removed in vacuo. The product was dissolved in 5 mL of ddH_2O to give 35 mmol (88% yield): ^{1}H NMR (500 MHz, D_2O, selected peaks) δ 7.75 (d, J = 7.7 Hz, 1H), 6.09 (t, J = 7.2 Hz, 1H), 6.02 (d, J = 7.3 Hz, 1H), 4.33−4.40 (m, 1H), 4.21−4.26 (m, 1H), 4.10−4.14 (m, 1H), 4.03−4.06 (m, 1H); ^{31}P NMR (121.5 MHz, D_2O, phosphoric acid external reference) δ −9.3, −10.5, −21.4.

[1′-^{2}H]F_2C. The synthesis of **8** was repeated with the substitution of NaB^2H_4 (98% ^{2}H, Sigma) for $NaBH_4$. The yield of [1′-^{2}H]F_2C (274 mmol) was 64%. The level of incorporation of ^{2}H was 93% as determined by ^{1}H NMR and ESI-MS. The corresponding mono-, di-, and tri-phosphates were prepared enzymatically in 86, 60, and 76% yield, respectively.

[1′-^{3}H]F_2CTP. Enzymatic phosphorylations to the mono-, di-, and triphosphates were conducted as described above to give 85% (SA of 8700 cpm/nmol), 60% (SA of 8620 cpm/nmol), and 88% (SA of 8620 cpm/nmol), respectively.

[5-^{3}H]F_2CTP. [5-^{3}H]F_2CDP was synthesized from [5-^{3}H]-F_2C provided by Eli Lilly (*30*). [5-^{3}H]F_2CDP (2.2 μmol) was converted to the triphosphate by the PEP/pyruvate kinase procedure described above. The yield was 1.85 mmol (85%) with a SA of 10060 cpm/nmol.

RTPR Assay (*spectrophotometric*). The assay mixture contained, in a final volume of 500 μL, RTPR (typically 0.25, 0.5, or 1 μM), CTP (1 mM), dATP (100 μM), NADPH (0.2 mM), TR (20 μM), TRR (0.2 μM), HEPES (25 mM, pH 7.5), EDTA (4 mM), and $MgCl_2$ (1 mM). The reaction was initiated with AdoCbl (20 μM) at 37 °C and monitored by the change in A_{340} (ε = 6220 M^{-1} cm^{-1}). The SA of RTPR was typically 0.28−0.44 mmol mg^{-1} min^{-1}.

RTPR Assay for Monitoring [^{14}C]dCTP. The assay mixture contained, in a final volume of 300 μL, RTPR (1 μM), [^{14}C]CTP (SA of 1500−2500 cpm/nmol, 1 mM), dATP (100 μM), NADPH (1 mM), TR (20 μM), TRR (0.2 μM), HEPES (25 mM, pH 7.5), EDTA (4 mM), and $MgCl_2$ (1 mM). The reaction was initiated with AdoCbl (20 μM) and the mixture incubated at 37 °C; a control aliquot was removed before addition of AdoCbl. Four aliquots (50 μL) were removed at time points over 5 min, and the reaction was quenched by addition of 2% perchloric acid (25 μL). The aliquots were neutralized with 0.4 M KOH (25 μL) after all time points were collected. Cytosine (50 nmol) and dC (50 nmol) were added to each aliquot; 20 units of alkaline phosphatase in 500 mM Tris (pH 8.6) and 1 mM EDTA (26.5 μL) was added, and the aliquots were incubated for 2 h at 37 °C. The dCDP was quantitated by the method of Steeper and Steuart (*41*).

Time-Dependent Inactivation of RTPR with F_2CTP (19, 21). The inactivation mixture contained, in a final volume of 100 μL, prereduced RTPR (5 μM), dATP (100 μM), NADPH (1 mM), TR (20 μM), TRR (0.2 μM), AdoCbl (20 μM), HEPES (25 mM, pH 7.5), EDTA (4 mM), and $MgCl_2$ (1 mM). To study inactivation in the absence of reductant, NADPH, TR, and TRR were omitted. The inactivation was initiated by addition of F_2CTP (or isotopically labeled derivative, 5 μM) and the reaction conducted at 37 °C. The assay for activity was conducted by measuring [^{14}C]dCTP production.

Size Exclusion Chromatography (*SEC*) *on RTPR Inactivated with [1′-^{3}H] or [5-^{3}H]F_2CTP*. Inactivation mixtures were prepared as described above in a final volume of 500 μL. Experiments were conducted both in the presence and in the absence of reductants. Inactivations were initiated by addition of F_2CTP (1′-^{3}H-labeled, SA of 7200 cpm/nmol; or 5-^{3}H-labeled, SA of 10800 cpm/nmol) and incubated for 2 min at 37 °C. An aliquot was assayed for activity using the spectrophotometric assay before initiation and at the inactivation end point. After 2 min, an aliquot (200 μL) was loaded on Sephadex G-50 columns (1 cm × 20 cm, 20 mL), equilibrated with and eluting with 25 mM HEPES (pH 7.5), 1 mM $MgCl_2$, and 4 mM EDTA, and 1 mL fractions were collected. A second aliquot (210 μL) was mixed with 630 μL of 8 M guanidine and then loaded on a Sephadex G-50 column (1 cm × 20 cm, 20 mL) equilibrated in and eluted with 2 M guanidine in assay buffer, and 800 μL fractions were collected. In all cases, fractions were assayed for A_{260} and A_{280} and for radioactivity by scintillation counting (500 μL aliquots). The recovery of radioactivity was typically >95%. The recovery of protein determined from A_{280} was typically >90%.

Elimination of Cytosine Deaminase Activity from Prereduced RTPR. An RTPR stock solution (~1 mM, 250 μL) was mixed with 5 mM *o*-phenanthroline (750 μL), and DTT was added to a final concentration of 30 mM. The solution was incubated for 20 min at 37 °C, and RTPR was isolated by Sephadex G-25 chromatography and quantified by standard procedures. Alternatively, the cytosine deaminase was removed by SEC on a Sephacryl S-300 column.

Spectrophotometric Detection of Cytosine Deaminase Activity in the RTPR Preparation. The conversion of cytosine (λ_{max} = 269 nm) to uracil (λ_{max} = 258 nm) was monitored spectrophotometrically. The reaction mixture contained, in a volume of 500 μL, 50 μM cytosine, 5 μM RTPR, 20 μM AdoCbl, 5 mM DTT, 25 mM HEPES (pH 7.5), 1 mM $MgCl_2$, and 4 mM EDTA. Three different preparations of RTPR were assayed: as isolated, purified by S-300 SEC, or pretreated with 3 mM *o*-phenanthroline. The UV spectra were recorded after 0 min, 30 min, 1 h, 6 h, and 1 day.

Analysis of Cytosine Generated during the Inactivation of RTPR with F_2CTP. The reaction mixture contained, in a final volume of 220 μL (or 1020 μL), prereduced RTPR (50 μM), dATP (500 μM), AdoCbl (50 μM), HEPES (25 mM, pH 7.5), EDTA (4 mM), and $MgCl_2$ (1 mM). [5-^{3}H]F_2CTP (50 μM, 7200 cpm/nmol) or [5-^{3}H]F_2CTP (50 μM, 10800 cpm/nmol) was added to initiate the reaction, and the mixture was then incubated for 2 min at 37 °C. Before initiation with F_2CTP and after the inactivation was complete, 10 μL aliquots were removed and assayed for RTPR activity by the spectrophotometric assay. At 2 min, the inactivation mixture was filtered through a YM-30 membrane (30000 molecular weight cutoff minicon) for 10 min at 14000*g* and 4 °C. F_2C (50 nmol) and cytosine (50 nmol) were added as carriers before filtration. Twenty units of alkaline phosphatase was added to the filtrate, and the reaction mixture was incubated for 3 h at 37 °C and filtered again using a YM-30 centricon.

The sample was then purified by HPLC using a Rainin SD-200 HPLC system and an Altech Adsorbosphere Nucleotide Nucleoside C-18 column (250 mm × 4.6 mm) with elution at a flow rate of 1 mL/min. The solvent system consisted of buffer A [10 mM NH_4OAc (pH 6.8)] and buffer B (100% methanol). The flow program was 100% A for 10 min followed by a linear gradient to 40% B over 25 min and then to 100% B over 5 min. Under these conditions, standards eluted as follows: cytosine at 5.7 min, uracil at 7.9 min, C at 12.6 min, *ara*-C at 17.4 min, dC at 19.0 min, and F_2C at 23.2 min. Fractions (1 mL) were collected; for samples with radiolabeled F_2CTP, 200 μL of each fraction was analyzed by scintillation counting. The cytosine peak was isolated and recovery calculated on the basis of the carrier added and scintillation.

Stability of [^{3}H]RTPR Generated by Inactivation with [1′-^{3}H]F_2CTP to Trypsin Digestion Conditions. The mixture contained, in a final volume of 300 μL, prereduced RTPR (15 μM), dATP (100 μM), AdoCbl (22.5 μM), HEPES (25 mM, pH 7.5), EDTA (4 mM), and $MgCl_2$ (1 mM). The reaction was initiated by addition of [1′-^{3}H]F_2CTP (SA 7200 cpm/nmol) to a final concentration of 15 μM. The reaction mixture was incubated for 2 min at 37 °C. The mixture, a 200 μL aliquot, was passed through Sephadex G-50 columns (1 cm × 20 cm, 20 mL) equilibrated and eluted in 0.1 M NH_4HCO_3 (pH 8) and 2 M urea (trypsin digestion buffer), and the protein-containing fractions were assayed for A_{280} and radioactivity. The sample (1.5 mL) was loaded into a Slidalizer dialysis cassette (10000 molecular weight cutoff) and dialyzed against the same buffer in which the sample was eluted. Aliquots (250 μL) were removed at 1, 2, 4, and 6 h. The dialysis buffers were changed, and the samples were dialyzed for an additional 14 h. A final aliquot was removed, and all aliquots were assayed for radioactivity by scintillation counting.

Trypsin Digestion of RTPR Inactivated with [1′-^{3}H]F_2CTP. The reaction mixture contained, in a final volume of 220 μL, prereduced RTPR (50 μM), dATP (500 μM), AdoCbl (75 μM), HEPES (25 mM, pH 7.5), EDTA (4 mM), and $MgCl_2$ (1 mM). [1′-^{3}H]F_2CTP (50 μM, SA of 7200 cpm/nmol) was added to initiate the reaction, and the reaction mixture was incubated for 2 min at 37 °C. Before initiation with F_2CTP and after the inactivation was complete, 10 μL aliquots were removed and assayed for RTPR activity. At 2 min, the inactivation mixture was quenched with 50 μL of 250 mM $NaBH_4$ and 400 mM Tris (pH 8.3) and incubated for an additional 5 min at 37 °C. The $NaBH_4$ solution was prepared via combination of solid $NaBH_4$ with the buffer solution immediately before use; vigorous foaming occurred upon addition to the inactivation mixture. To this mixture was added 750 μL of 8 M guanidine, 40 mM DTT, 5.33 mM EDTA, and 400 mM Tris (pH 8.3), and the reaction mixture was incubated for 30 min at 37 °C. Iodoacetamide was added to a final concentration of 250 mM (25000 equiv per RTPR) and the reaction mixture incubated for an additional 1 h at 37 °C. The protein was then separated from small molecules on a Sephadex G-50 column (1 cm × 20 cm, 20 mL) equilibrated into 0.1 M NH_4HCO_3 (pH 8.2) [or 0.1 M NH_4HCO_3 (pH 8.2) and 2 M urea]. The protein-containing fractions were combined (typically 2 mL total volume, 90% recovery of protein, > 95% recovery of loaded radioactivity, 0.28 equiv of radioactivity coeluted with protein). Trypsin (Worthington) was added from a freshly prepared stock solution to a final RTPR:trypsin concentration ratio of 4:1 (w/w) and incubated for 2 h at 37 °C. The reaction was quenched by addition of 25 μL of trifluoroacetic acid (TFA, to pH ~2), and the peptides were immediately separated using a Waters 2487 HPLC system with a Phenomenex Jupiter C18 peptide column (150 mm × 4.6 mm, 5 μm, 300 Å pore size) at a flow rate of 1 mL/min. The peptides were eluted with buffer A (0.1% TFA in ddH_2O) and buffer B (0.1% TFA in acetonitrile) by a linear gradient from 0 to 45% B over 90 min. Fractions were collected (1 mL), and aliquots (100 μL) of each fraction were assayed for radioactivity by scintillation counting. The recovery of injected radioactivity was typically 80%. Four regions of radioactivity were observed (Figure 1). Fractions were pooled on the basis of the observed peaks of radioactivity, concentrated to < 1 mL on a lyophilizer, and repurified using the same column and flow rate with buffer A [10 mM NH_4OAc (pH 6.8)] and buffer B (100% acetonitrile) using a gradient from 0 to 35% B over 90 min. Fractions (1 mL) were collected, and aliquots of each fraction (250 μL) were assayed for radioactivity. The major peaks of radioactivity were pooled and submitted for mass spectrometry analysis without concentration. Reactions were also conducted as described above substituting NaB^2H_4 for $NaBH_4$ or F_2CTP that was a mixture of 1′-^{2}H- and 1′-^{3}H-labeled forms (SA of 7200 cpm/nmol) to give a stock with 60% 1′-^{2}H with a SA of 2600 cpm/nmol.

Peptide Mass Spectrometry (42). MALDI-TOF and tandem MS/MS mass spectrometry were performed by J. Leszyk at UMass Medical School on a Kratos Axima CFR (Shimadzu Instruments) matrix-assisted laser desorption ionization (MALDI) mass spectrometer. Samples (0.5 mL, containing 50−100 fmol of F_2CTP-labeled peptide, determined by specific activity) were applied to the target and mixed with 0.5 μL of matrix which was 2,5-dihydroxybenzoic acid at 15 mg/mL in a 50:50 CH_3CN/0.1%TFA mixture. Samples were allowed to air-dry prior to being inserted into the mass spectrometer. Peptides were analyzed in positive ion mode in midmass range (100−3000 Da) with an accuracy of ±100 ppm. The instrument was

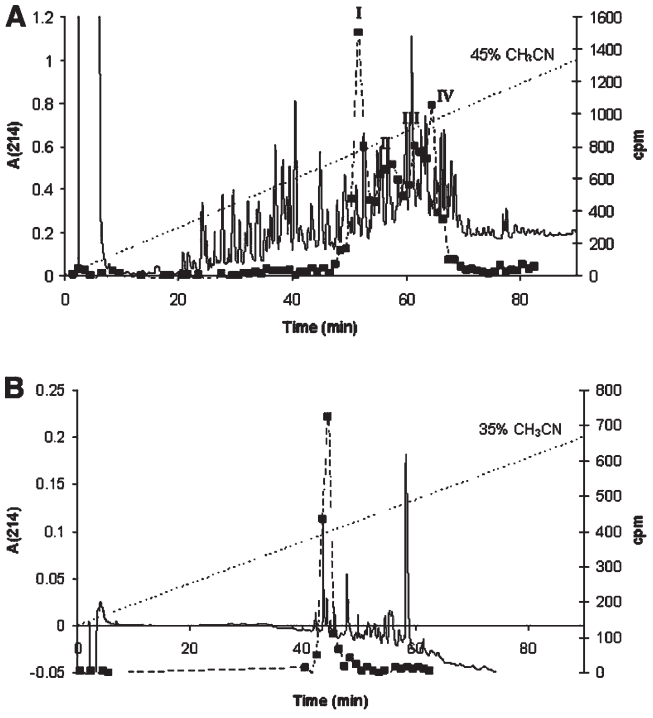

FIGURE 1: HPLC purification of peptides from RTPR inactivated with [1′-^{3}H]F_2CTP, treated with $NaBH_4$ at 2 min, alkylated with iodoacetamide, and digested with trypsin. A_{214} (—) and counts per minute (---). (A) Initial purification with a linear gradient (···) with 0.1% TFA from 0 to 45% CH_3CN over 90 min: region I, 50−53 min, 18.1% of radioactivity; region II, 54−59 min, 19.7% of radioactivity; region III, 60−63 min, 13.9% of radioactivity; region IV, 63−67 min, 26% of radioactivity. (B) Repurification of region I with a linear gradient (···) with 10 mM NH_4OAc (pH 6.8) from 0 to 35% CH_3CN over 90 min (80% recovery of radiolabel).

externally calibrated with bradykinin (757.40 Da), P14R (MS mass standard, Sigma-Aldrich, 1533.86 Da), and adrenocorticotropic hormone fragment 18−39 (Sigma-Aldrich, 2465.20 Da). Post-source decay (PSD) analysis was performed on the same instrument using a timed ion gate for precursor selection with a laser power ~20% higher than that for MS acquisition. PSD fragments were separated in a curved field reflectron that allowed for a seamless full mass range acquisition of the spectrum, with an accuracy of ±1000 ppm. All spectra were processed with Mascot Distiller (Matrix Sciences, Ltd.) prior to database searching (*43*). Database searches were performed with Mascot (Matrix Sciences, Ltd.). For MS searches, the Peptide Mass Fingerprint program was used with a peptide mass tolerance of 150 ppm. For MS/MS searching, the MS/MS Ion Search program was used with a precursor tolerance of 150 ppm and a fragment tolerance of 1 Da.

SDS−PAGE of RTPR Inactivations with F_2CTP. Inactivations were performed as described above. Each sample contained, in a final volume of 300 μL, prereduced RTPR (25 μM), dATP (500 μM), AdoCbl (37.5 μM), HEPES (25 mM, pH 7.5), EDTA (4 mM), and $MgCl_2$ (1 mM). The reaction was initiated by addition of F_2CTP to a final concentration of 25 μM. Reaction mixtures containing reductant used 5 mM DTT. Aliquots were quenched when mixed with an equal volume of 2× Laemlli buffer. An aliquot was removed immediately after F_2CTP addition (0 min), and two aliquots were removed at 5 min: one was not boiled, and the other was boiled for 3 min. Samples were analyzed on a 10% SDS−PAGE gel and band intensities measured. The band intensities were quantified using Bio-Rad Quantity One.

SEC on C119S RTPR Inactivated with [1′-^{3}H]F_2CTP. SEC experiments were performed with C119S-RTPR, which was analyzed as described above for wild-type RTPR in the absence of reductants.

Characterization of Major Nucleoside Product(s) Isolated from a $NaBH_4$-Quenched $C_{119}S$ RTPR/F_2CTP Inactivation Mixture. The reaction mixture contained, in a final volume of 200 μL, C119S-RTPR (50 μM), dATP (250 μM), AdoCbl (75 μM), F_2CTP (50 μM), HEPES (25 mM, pH 7.5), EDTA (4 mM), and $MgCl_2$ (1 mM). The inactivation reaction was quenched at 2 min with 50 μL of 250 mM $NaBH_4$ in 500 mM Tris (pH 8.5) in a 4.0 mL Falcon tube and the mixture incubated for 5 min at 37 °C. The $NaBH_4$ solution was prepared by using solid $NaBH_4$ as described above. The solution was then filtered through a YM-30 membrane for 15 min at 14000*g* and 4 °C, and the flow-through was treated with 200 units of alkaline phosphatase for 3 h at 37 °C, followed by filtration through a second YM-30 membrane. The sample was acidified by addition of glacial acetic acid (5% of the final volume), and the resulting mixture was lyophilized to dryness to hydrolyze borate esters. The residue was then taken up in 1 mL of 10 mM NH_4OAc and purified on an Altech Adsorbosphere Nucleotide Nucleoside C-18 column (250 mm × 4.6 mm) using a 2 mL injection loop with elution at a flow rate of 1 mL/min. The solvent system for elution and analysis of nucleosides was described above for cytosine identification. Fractions were collected (1 mL), and aliquots (100 μL) of each fraction were assayed for radioactivity by scintillation counting. The major peak of radioactivity (43% of total counts) was found to co-elute with a standard of 2′-fluoro-2′-deoxycytidine. The presence of this compound was confirmed: ESI-MS ($C_9H_{12}FN_3O_4$) *m*/*z* ($M + Na^+$) calcd 268.0710, observed 268.0718; ($M + H^+$) calcd 246.0890, observed 246.0901.

RESULTS

Synthesis of Isotopically Labeled F_2CTP. The synthesis of [1′-^{3}H]F_2C (**10**) was conducted using modifications of the previously published procedure and is summarized in Scheme S1 of the Supporting Information (*34*). The reduction of the difluorinated lactone **6** used disiamylborane made from NaB^3H_4 and 2 methyl-2-butene. The presence of the two fluorines required an increased ratio of disiamylborane to **6** relative to ribonolactone to produce high yields (*36*). The reduced **7** was then converted directly to the mesylate **8** with mesyl chloride and TEA without purification in 85% yield from the lactone **6**. The mesylate was coupled to bis-trimethylsilylcytosine **9** prepared by refluxing cytosine in a 10:1 HMDS/TMSCl mixture. Efforts to make **9** from cytosine in HMDS using ammonium sulfate as a catalyst were unsuccessful on the small scale used to make [1′-^{3}H]F_2C. **9** added to **8** in xylenes and refluxed in the presence of trimethylsilyl trifluoromethanesulfonate resulted in production of protected nucleoside as a 6:4 α/β mixture that was directly deprotected with sodium methoxide to give α/β **10** in 74% yield from **8**. The published protocols separate the F_2C anomers by crystallization at either the benzoate-protected or fully deprotected stage. This approach is incompatible with the scale used for radiolabeled syntheses. After investigating a number of options, we determined that it is most convenient to resolve the α/β mixture enzymatically during the conversion of F_2C to F_2CMP.

Phosphorylation of F_2C. F_2C is very difficult to phosphorylate chemically using activated phosphates due to the enhanced acidity of its 3′-OH which results in rapid formation of the 3′,5′-cyclic phosphate. Previous studies had reported the ability to generate F_2CMP using human dCK and to generate F_2CDP using F_2CMP and UMP/CMP kinase (*6*, *42*, *43*, *47*−*49*). Treatment of α/β-F_2C with human dCK and ATP allowed selective conversion of the β anomer to the 5′-monophosphate (F_2CMP) in 85% yield. The desired product readily separated from the remaining nucleoside during anion exchange chromatography.

To make the F_2CTP, we first made the F_2CDP, which also has been used to investigate the class I RNRs which use NDP substrates. F_2CDP was generated enzymatically from F_2CMP and ATP with human UMP/CMP kinase. However, this procedure yields an equilibrium mixture of starting material and products: F_2CDP and ADP. Since these products co-elute on anion exchange chromatography, a periodate cleavage step was introduced to destroy ADP (*30*, *40*). $NaIO_4$ (aqueous) selectively reacts with the *syn*-diol of the ADP to cleave the 2′-C−3′-C bond generating a dialdehyde. The F_2CDP is unreactive. After removal of excess periodate, $MeNH_2$ (pH 7.5) is added to catalyze elimination of pyrophosphate from the dialdehyde. Addition of inorganic pyrophosphatase converts the inorganic pyrophosphate to inorganic phosphate. Anion exchange chromatography of this reaction mixture allows recovery of homogeneous F_2CDP in 56% yield.

In the development of the UMP/CMP kinase procedure for production of F_2CDP, experiments were initially conducted in the presence of pyruvate kinase and PEP to recycle the ADP to ATP and prevent the problem of its separation from F_2CDP (*30*). However, HPLC analysis indicated that the F_2CDP was phosphorylated under the conditions investigated. This observation suggested that pyruvate kinase could be used to make F_2CTP. Two equivalents of PEP and 120 units/mL pyruvate kinase resulted in 88% conversion to F_2CTP in 1 h. The enzymatic phosphorylation methods have been used to prepare all of the isotopically labeled gemcitabine nucleotides [[5-^{3}H]$F_2CD(T)P$ and [1′-^{2}H]$F_2CD(T)P$] in 10−100 μmol quantities.

Covalent Labeling of RTPR by [1′-^{3}H]- and [5-^{3}H]-F_2CTP. Our previous studies suggested that 1 equiv of F_2CTP was sufficient for 90% inactivation of RTPR within 30 s in the presence and absence of reductants (TR, TRR, and NADPH), and 95% by 2 min (*21*). At that time, we suggested that inactivation might in part result from covalent labeling of RTPR and in part from covalent labeling of C_{419} by a cobalamin species (*21*). The availability of [1′-^{3}H]- or [5-^{3}H]F_2CTP has now allowed us to test these proposals by tracking the fate of the ribose ring in the case of [1′-^{3}H]F_2CTP and the cytosine base in the case of [5-^{3}H]F_2CTP. RTPR was incubated with these compounds for 2 min, and the small molecules were separated from the protein by SEC in the presence or absence of denaturant. The results are summarized in Table 1. With [1′-^{3}H]F_2CTP, 0.47 ± 0.02 equiv co-elutes with RTPR in both cases. With [5-^{3}H]F_2CTP, only 0.16 equiv co-elutes with RTPR in the presence and absence of reductants, with a slight reduction in recovered label under denaturing conditions. The substoichiometric labeling, the >90% inactivation, and the observation that C_{419} can be modified with the corrin of AdoCbl suggest a branching mechanism for inactivation of RTPR (*21*).

Release of Cytosine Accompanies Inactivation. It was surprising that there was significantly less cytosine bound to RTPR than ribose (Table 1), as our earlier studies failed to detect any cytosine subsequent to the inactivation (*21*). Given our results with [5-^{3}H]F_2CTP and the observation that cytosine is released when the class I RDPRs from *E. coli* or human are inactivated with F_2CDP (*20*, *23*−*25*), our efforts focused on determining if cytosine was being converted to uracil. The inactivation was conducted with [5-^{3}H]F_2CTP, and the small molecules were analyzed by RP-HPLC subsequent to dephosphorylation of the nucleotides with alkaline phosphatase. The retention time of the new ^{3}H-labeled material was identical to that of a uracil standard. Isolation of this material and examination by UV and NMR spectroscopy confirmed its identity. These results suggested that RTPR preparations were contaminated with *E. coli* cytosine deaminase (*44*). Several different types of experiments confirmed this to be the case and allowed its removal (see Materials and Methods). Inactivation studies with [5-^{3}H]F_2CTP were then repeated and the small molecules analyzed by HPLC subsequent to dephosphorylation. When we started with a 1:1 ratio of [5-^{3}H]F_2CTP to RTPR, 0.71 equiv of cytosine and 0.19 equiv of unreacted F_2C were recovered. In addition, 0.15 equiv of cytosine co-eluted with RTPR, accounting for all of the radiolabel.

Identification of Peptide or Peptides of RTPR Labeled during Its Inactivation with F_2CTP and Insight into the Structure of the Sugar Moiety or Moieties Responsible for Labeling. As summarized in Table 1, 0.47 ^{3}H labels from [1′-^{3}H]F_2CTP was found covalently attached to RTPR and is likely associated with the loss of 47% of the RTPR activity. Subsequent to inactivation of RTPR by [1′-^{3}H]F_2CTP, the protein was denatured in 8 M guanidine and the cysteines were alkylated with iodoacetamide. The alkylated RTPR was exchanged into the trypsin digest buffer [0.1 M NH_4HCO_3 (pH 8.2)] by Sephadex G-50 chromatography, and the protein-containing fractions were pooled and analyzed for protein and radioactivity. While 80% of the protein was recovered, only 0.14 equiv of radioactivity co-eluted with the protein, indicating substantial loss of the label during the denaturation and iodoacetamide treatment. Furthermore, when the ^{3}H-labeled RTPR was digested with trypsin and the peptides were separated by reverse-phase HPLC, 10% of the radioactivity eluted in the void volume of the column and the remaining radioactivity eluted in a very broad peak between 45 and 65 min (data not shown). These results suggested that inactivation results in multiple sites of labeling or more likely that the label is redistributed to multiple residues during the workup.

Our previous experience with identifying the site of attachment of the label to RTPR inactivated by the mechanism-based inhibitor, [2′-^{3}H]-2′-chloro-2′-deoxynucleotide (Scheme 2), suggested that the loss of label might be minimized by reduction with $NaBH_4$. Thus, subsequent to inactivation, the reaction mixture was treated with 50 mM $NaBH_4$. The labeled RTPR that was recovered (Table 1) was reduced from 0.45 to 0.33 equiv. Under the conditions of alkylation, trypsin digestion, and HPLC purification of the resulting peptides, 0.22 equiv of radiolabel was recovered. The results of a typical chromatography are shown in Figure 1 where four main regions of radioactivity are identified. The average total recovery of radiolabel from column chromatography from six experiments was 74 ± 5%, with 20 ± 2% in region I, 26 ± 4% in region II, 20 ± 5% in region III, and 21 ± 4% in region IV.

Fractions from each region of the chromatogram were pooled and rechromatographed at pH 6.4 in potassium phosphate buffer. The results from region I are shown in Figure 1B. Regions

Table 1: Covalent Labeling of RTPR with [1′-^{3}H]- and [5-^{3}H]F_2CTP

enzyme	F_2CTP label	TR, TRR, and NADPH	Sephadex G-50[a]	label eluting with protein (equiv/RTPR)
wild type	1′-^{3}H	+	native	0.46
wild type	1′-^{3}H	−	denaturing	0.47
wild type	1′-^{3}H	−	native	0.49
wild type	1′-^{3}H	−	denaturing	0.44
wild type, $NaBH_4$ at 2 min	1′-^{3}H	−	native	0.33
wild type	5-^{3}H	+	native	0.17
wild type	5-^{3}H	+	denaturing	0.13
wild type	5-^{3}H	−	native	0.15[b]
wild type	5-^{3}H	−	denaturing	0.12
wild type, $NaBH_4$ at 2 min	5-^{3}H	−	native	0.03

[a]Under denaturing conditions, 6 M guanidinium hydrochloride was added to the inactivation mixture before it was loaded onto the Sephadex column and the column was eluted with 2 M guanidinium hydrochloride. [b]Under these conditions, the small molecules were dephosphorylated and analyzed by HPLC and 0.71 equiv of cytosine and 0.18 equiv of F_2C were found.

Scheme 2: Proposal for Structures That Can Be Accommodated by the Labeling Observed in the MS Data

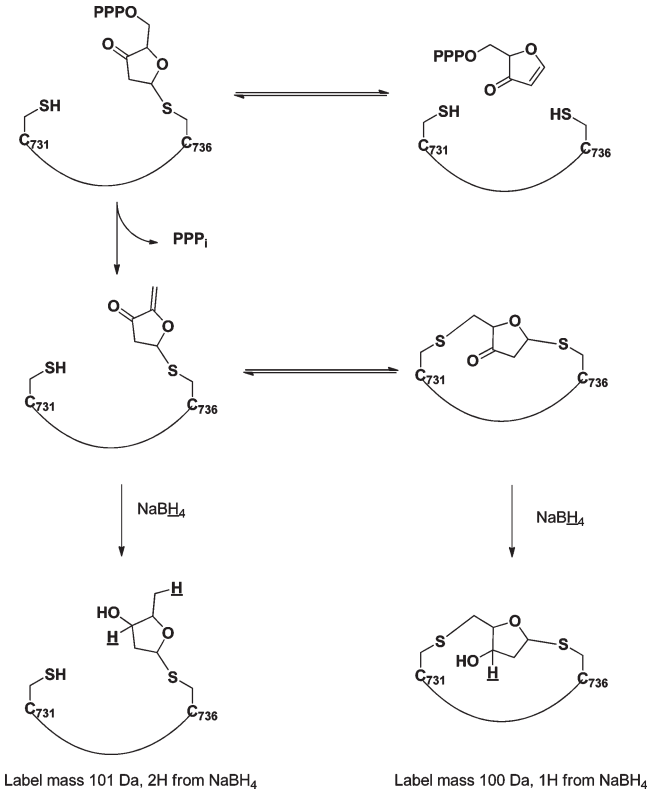

II−IV were also rechromatographed (data not shown). All label was lost from region IV (*45*).

Analysis of the Labeled Peptide Isolated from Region I by MALDI-TOF Mass Spectrometry. MALDI analysis was performed on the peptides isolated from region I (Figure 2A−C and Figure 3A,B) and regions II and III (data not shown). To facilitate identification of peptides containing a sugar fragment derived from F_2CTP, two additional experiments were conducted. In one set of experiments, [1′-^{2}H,^{3}H]F_2CTP with ~60% ^{2}H at the 1′ position and a specific activity of 2600 cpm/nmol was used for the inactivation, and in the second set of experiments, NaB^2H_4 replaced $NaBH_4$. Inactivation reactions involving these changes will result in the same, labeled peptides, but with additional mass and a predictable mass distribution. When using F_2CTP partially labeled with ^{2}H, any peptides incorporating the sugar ring of F_2CTP show an isotopic

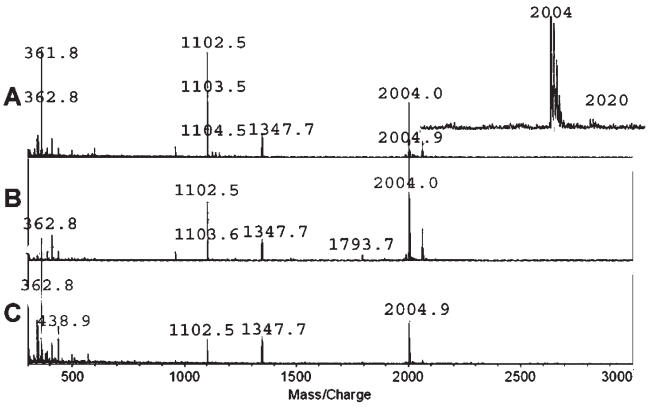

FIGURE 2: Full MALDI-TOF analysis of the peptides isolated in region I from the trypsin digest of RTPR inactivated with F_2CTP and treated with $NaBH_4$: (A) [1′-^{3}H]F_2CTP with $NaBH_4$, (B) [1′-^{2}H,^{3}H]F_2CTP with $NaBH_4$, and (C) [1′-^{3}H]F_2CTP with $NaBD_4$. The features at 1102.5 and 1347.7 Da are not from RTPR, as MS/MS fragmentation analysis showed no matches with sequences from RTPR. The inset shows a zoom of spectrum A around the 2004 Da peak to highlight the presence of a peak at 2020 Da.

distribution shifted such that the 1 Da peak increases in intensity [Figure 2B, Figure 3A (II), and Figure 3B (II)], allowing confirmation of the source of the label. Alternatively, the experiments quenched with NaB^2H_4 will show a shift of *x* Da over the peptides quenched with $NaBH_4$ [Figure 2C, Figure 3A (III), and Figure 3B (III)], where *x* indicates the number of hydrogens in the label originating from the borohydride quench.

The MALDI spectra of the peptides isolated from region I under the three sets of conditions are shown in Figures 2A−C and 3A,B. Two peptides, one with a mass of 2004 Da and one with a mass of 2063 Da, show shifts in isotopic distribution from the nondeuterated material [compare Figure 3A (I) with Figure 3A (II and III) and Figure 3B (I) with Figure 3B (II and III)]. No peptides from regions II and III (Figure 1) showing the shift in isotopic distribution were detected in the MALDI analysis, despite these regions representing a substantial percentage of the radioactivity recovered from the trypsin digests. We propose the lack of identifiable labeled peptides is due to a combination of a number of potential cross-linked species with a low incidence of each specific sequence (see the discussion of the mechanism below) and that some of these cross-linked peptides might be too large to be seen in the high-resolution MALDI experiments.

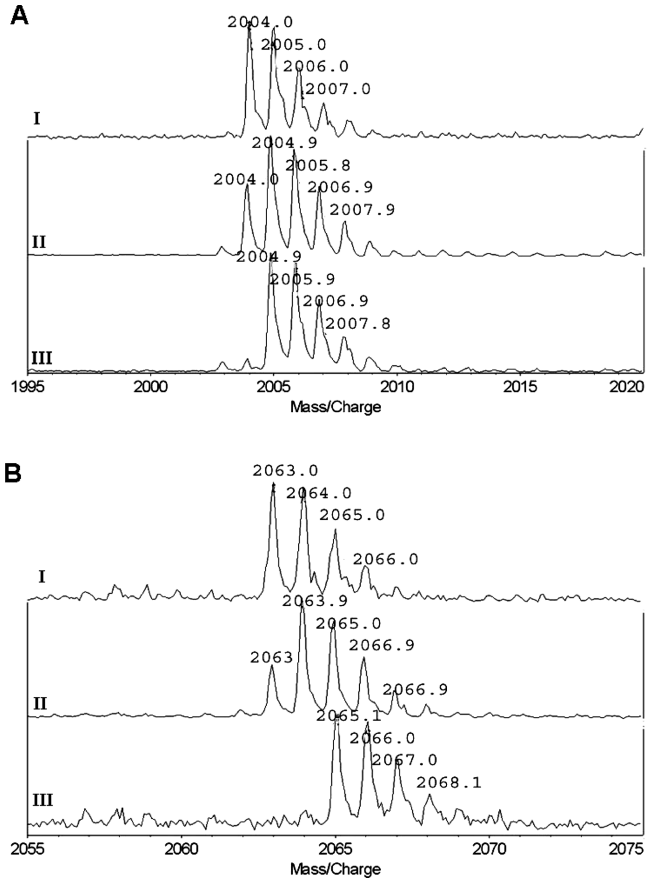

FIGURE 3: (A) Expansion of the MALDI spectrum in Figure 2 in the region around the 2004 Da peak: (I) [1′-^{3}H]F_2CTP with $NaBH_4$, (II) [1′-^{2}H,^{3}H]F_2CTP with $NaBH_4$, and (III) [1′-^{3}H]F_2CTP with $NaBD_4$. (B) Expansion of the MALDI spectrum in Figure 2 in the region around the 2063 Da peak: (I) [1′-^{3}H]F_2CTP with $NaBH_4$, (II) [1′-^{2}H,^{3}H]F_2CTP with $NaBH_4$, and (III) [1′-^{3}H]F_2CTP with $NaBD_4$.

Our previous studies with RTPR inactivated by [2′-^{3}H]-2′-chloro-2′-deoxy-UTP followed by $NaBH_4$ trapping identified alkylation of cysteines within the C-terminus of RTPR (*46*). The C-terminal tail contains a pair of cysteines (C_{731} and C_{736}) essential to the function of the enzyme, re-reducing the active site disulfide formed after every nucleotide reduction (*47*−*50*). The expected mass of this C-terminal peptide with both cysteines [C_{731} and C_{736} within the peptide of residues 722−739 (D_{722}LELVDQTDCEGGACPIK_{739})] labeled with acetamide is 2019.90 Da and should be present in our digests if this region is alkylated. This peptide is detected at 2020.04 Da (Figure 2, inset) and serves as an internal control for the identification of C-terminal peptides labeled with F_2CTP derivatives.

Since one or both of these cysteines could be the site of alkylation, the labeled peptide could be missing one or both acetamides [loss of one or two 58 Da adducts gives rise to 2020 − 2 (58) = 1904 Da or 2020 − 58 = 1962 Da species]. If both acetamides are missing, a sugar moiety from F_2CTP would need to have a mass of 100 Da (1904 + 100 = 2004) to give the observed mass of 2004 Da. Alternatively, if the peptide at 2063 Da corresponds to the C-terminal peptide with one acetamide, then the group derived from F_2CTP would have a mass of 101 Da (1904 + 58 + 101 = 2063).

To learn more about the structure of the labeled species and the number of hydrogen atoms derived from $NaBH_4$, the inactivation mixture with [1′-^{3}H]F_2CTP and NaB^2H_4 (98% D) was examined. Trapping with NaB^2H_4 can occur by 1,2-reduction of a ketone or the 1,4-reduction of an unsaturated ketone (Scheme 2). In either case, the observed mass of the adduct would result in the addition of 1 Da. In addition, the ketone subsequent to 1,4-reduction could then itself be reduced, resulting in the incorporation of a second deuterium (+2 Da). The analysis of peptides isolated subsequent to this treatment is shown in Figure 2C, Figure 3A (III), and Figure 3B (III).

In the expansion of the 2004 Da peak (Figure 3A), the mass of the peptide shifts from 2004 to 2005 Da after $NaB[^2H]_4$ trapping [Figure 3A (I and III)]. In the expansion of the 2063 Da peak (Figure 3B), the mass is shifted by 2 Da to 2065 Da [Figure 3B (I) and Figure 3B (III)]. These results establish that one hydrogen in the species with a mass of 2004 Da and two hydrogens in the species with a mass of 2063 Da come from $NaBH_4$.

Analysis by MS/MS. To gain more information about the structure of the modification(s), the sequence of the peptide, and the residues alkylated, MS/MS analysis was performed. The initial focus was on the peptide with a mass of 2020 Da (Figure 2A, inset) where the mass itself is consistent with two cysteines modified by acetamide. This assignment was confirmed by post-source decay (PSD) fragmentation (Figure S1 of the Supporting Information). In this method, additional energy is applied to the peptide of interest, initiating predictable fragmentation patterns. The major site of fragmentation is at peptide bonds and gives rise to two series of ions: the y series in which the charge is retained on the N-terminus and the b series with the charge retained on the C-terminus (Scheme S2 of the Supporting Information) (*51*, *52*). Each mass peak within a given series is thus associated with a truncated peptide, and the difference in mass between each peak within a given series is the mass of one amino acid in the sequence. The relative abundance of each ion series detected is highly peptide dependent, and in the case of the 2020 Da peptide (Figure S1 of the Supporting Information), the y series dominates the spectrum. A number of additional peaks can be seen that are −18 and −17 Da from the main y series. These are the y^0 and y* series, representing loss of water and ammonia, respectively, from the y series ions. The peaks from the major "y" series are marked (vertical line), and the difference in mass indicates the amino acid lost, allowing sequencing of the peptide. Most remaining peaks visible in the spectrum are b series peptides. This spectrum allows N-terminal sequencing by viewing the y series. Fourteen y ions are observable, showing mass differences consistent with the C-terminal RTPR peptide, with both cysteines modified by acetamide.

The MS/MS spectrum of the 2063 Da peptide shows the same series of ions as in the doubly acetamide-labeled C-terminal peptide (Figure S1 of the Supporting Information), but shifted by +43 Da (Figure 4). The same series is visible in the 2065 Da peptide from the NaB^2H_4-quenched reaction, but at +45 Da (data not shown). Once the first cysteine is removed, both the normal series seen in the MS/MS spectrum for the acetamide-modified peptide [peaks at 831, 702, 645, 588, and 517 Da (Figure 4)] and a series which remains at +43 Da (+45 Da for the NaB^2H_4-quenched reaction) can be seen. After the cleavage of the second cysteine, only the normal mass peak remains (a fragment at 357 Da). The label derived from the sugar fragment of F_2CTP is thus attached to either C_{731} or C_{736}. This method is not quantitative, and nothing can be said about the relative extent of labeling at each site. As predicted by MALDI, the sugar fragment has a mass of 101 Da (43 Da larger than that of acetamide) and incorporates two deuteriums when the inactivation is quenched with NaB^2H_4.

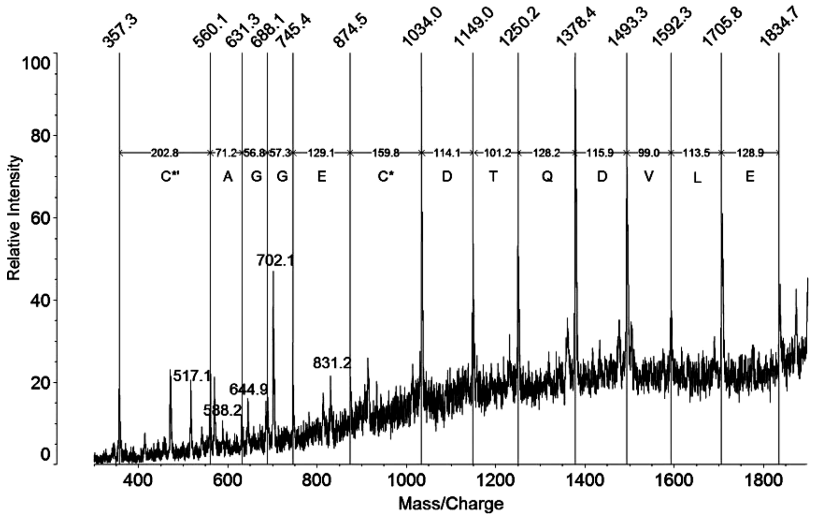

FIGURE 4: (A) MS/MS spectrum of the peak at 2063 Da, containing a label derived from F_2CTP. The y series is marked and corresponds to the C-terminal peptide of RTPR (DLELVDQTDCEGGACPIK). The absolute molecular masses detected are shifted +43 Da relative to the acetamide-labeled C-terminal peptide (Figure S1 of the Supporting Information), suggesting alkylation at cysteine by a group 43 Da larger than acetamide. The modification is present to some extent on each cysteine, as indicated by the appearance of the y series of the normal peptide after C_{731} is cleaved (indicated at 831, 702, 645, 588, and 517 Da).

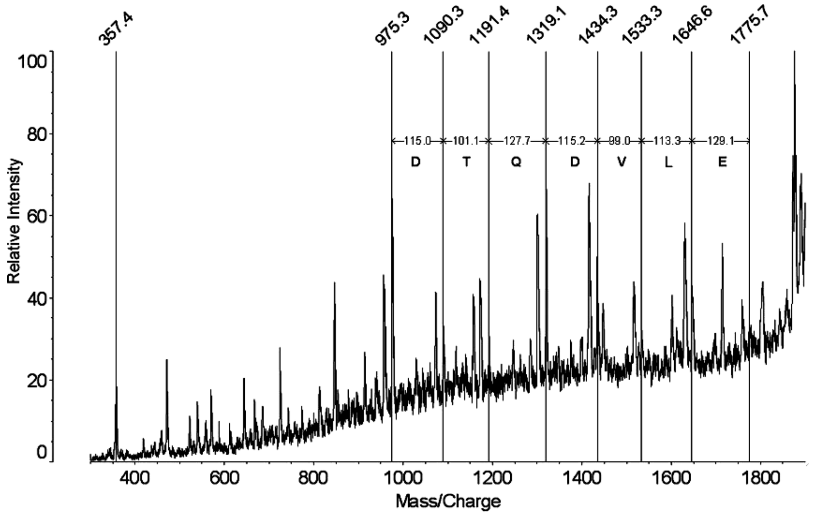

FIGURE 5: MS/MS spectrum of the peak at 2004 Da corresponding to the C-terminal peptide of RTPR (DLELVDQTDCEGGACPIK) containing an internal cysteine−cysteine cross-link derived from F_2CTP. The y ion series is indicated. No regular ions were detected in the mass range of 360−970 Da.

The MS/MS spectrum of the major labeled peak at 2004 Da is more complex than that at 2063 Da (Figure 5). The expected y series for the C-terminal peptide is still evident, −16 Da relative to the diacetamide-modified C-terminal peptide (Figure S1 of the Supporting Information). Each of these peaks shows several closely related series, fragments that are −17 or −18 Da relative to each y ion (the y* series that has lost ammonia and the y^0 series that has lost water) and often show a fragment at −35 Da, representing the loss of both water and ammonia. It is unclear why the intensities of these secondary fragments are enhanced relative to those of the corresponding series in the 2020 and 2063 Da (Figure 4) peptides. Additionally, after the loss of the aspartate before C_{731} (giving the peak at 975 Da), the peaks visible until the loss of the second cysteine do not correlate with any simple mass series. This result indicates some irregular fragmentation of the peptides in this mass range. The nature of this fragmentation is not readily apparent. The final tripeptide fragment after cleavage of C_{736} (PIK) is the same in this spectrum as in those for the 2020 and 2063 Da species. The PSD for the 2005 Da peak in the NaB^2H_4 spectra is similar, but shifted +1 Da relative to the 2004 Da spectra, and the primary y series is of even lower abundance relative to the y^0 and y* series (data not shown).

These data are consistent with modification at C_{731} and C_{736}. If both acetamides are missing, a fragment with a mass of 100 Da derived from F_2CTP would account for the observed mass ($2020 - 2 \times 58 + 100 = 2004$). Our interpretation of this data is that this modification is a 100 Da fragment that is covalently modifying both cysteines, providing an internal cross-link. Cleavages in the backbone between the two cysteines would not actually fragment the peptide if they were connected through a side chain cross-link and could account for the lack of regular fragments in this region.

Interpretation of MALDI and MS/MS Data. The peptides associated with masses at 2004 and 2063 Da represent cysteine-modified C-terminal peptides of RTPR. Modification is evident at both C_{731} and C_{736}. The mass at 2004 Da is consistent

with the replacement of both acetamides with a fragment of 100 Da that is covalently linked to both cysteines. The peptide at 2063 Da is consistent with the same peptide; however, it has one cysteine labeled with acetamide and one with a sugar fragment of 101 Da. The NaB^2H_4-quenched sample shows that one hydrogen on the 100 Da fragment comes from $NaBH_4$ and that two on the 101 Da fragment come from $NaBH_4$.

Scheme 2 outlines a model consistent with these data. A furanone equivalent could react with the C-terminal cysteines though conjugate addition, either with one cysteine leaving a compound with an α,β-unsaturated ketone or with both cysteines giving rise to a saturated ketone. Reduction with $NaBH_4$ would provide the structure with the correct mass and number of hydrogens delivered from $NaBH_4$. Other alternative schemes that can be envisioned are inconsistent with the NaB^2H_4 labeling experiment.

Change in the Conformation of RTPR Subsequent to Labeling by F_2CTP Determined by SDS−PAGE. Recent studies with of class Ia RNRs inactivated by F_2CDP and analyzed by SDS−PAGE subsequent to inactivation revealed that ~30% of the α migrated as a protein with a larger molecular mass (*23*−*25*). Inactivation reaction mixtures of RTPR were therefore analyzed by SDS−PAGE to detect any changes in conformation related to the inactivation process (Figure 6). Samples with and without DTT were analyzed at 0 and 5 min subsequent to the inactivation with and without boiling of the 5 min sample. All inactivations quenched at 5 min showed the presence of a new major band at ~100 kDa representing 25% of the overall intensity, with a corresponding reduction in the intensity of the wild-type RTPR band at 75 kDa. Assuming 75−80% of the RTPR is active (*47*, *53*−*55*), this new feature represents ~33% of the RTPR. We suggest that it is an altered protein conformation that is generated regardless of the presence or absence of DTT in the assay buffer or whether the sample is boiled prior to sample loading. Samples at 5 min also showed a second new minor band (< 5% intensity).

Inactivation of C119S-RTPR by [1′-^{3}H]F_2CTP. Studies of the class Ia RNRs suggested that an active site cysteine involved directly in nucleotide reduction (C_{225} in *E. coli* RNR) is alkylated by the sugar moiety of F_2CDP (*24*, *25*). C119S-RTPR, a mutant of the corresponding α face cysteine implicated in labeling in the class Ia RNR, was therefore inactivated by [1′-^{3}H]F_2CTP and analyzed by SEC. The results demonstrated 0.33 equiv of radiolabel co-eluting with the protein under denaturing conditions. This number contrasts with the 0.47 equiv labeling for the wild-type RTPR and suggests that this cysteine might in part represent a site of labeling, not identified in the peptide mapping analysis described above.

In a separate experiment, the small molecule fraction of the inactivation mixture with C119S-RTPR was examined, subsequent to quenching at 2 min with $NaBH_4$ to reduce any transient ketone-containing species. The phosphates of the nucleotides were removed with alkaline phosphatase, and the small molecules were analyzed by RP-HPLC. Three regions of radioactivity were identified: one broad region (15−19 min, 26% of the radioactivity) and two sharper peaks (22.2 min, 43% of the radioactivity, and 23.2 min, 11% of the radioactivity). The peak at 22.2 min co-eluted with 2′-deoxy-2′-fluorocytidine, while the peak at 23.3 min co-eluted with F_2C. The presence of a compound with a mass equal to that of 2′-fluorocytidine was confirmed by high-resolution ESI-MS for the 22.2 min peak. Trapping of this species has interesting mechanistic implications discussed below.

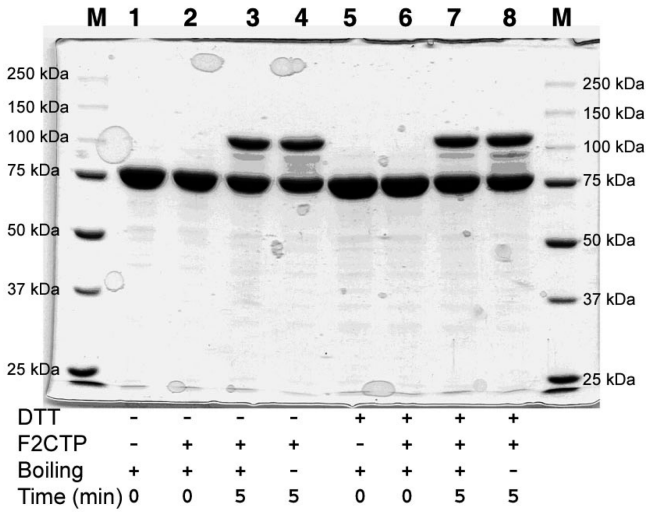

FIGURE 6: SDS−PAGE of RTPR inactivated by treatment with F_2CTP.

DISCUSSION

We previously reported SF kinetic experiments for the inactivation of RTPR with AdoCbl by F_2CTP. The results demonstrated that 0.7 equiv/RTPR of cob(II)alamin was formed with a k_{obs} of 50 s^{-1}. RFQ EPR experiments further revealed that cob(II)alamin was exchange coupled to a thiyl radical (1.4 spins/RTPR) and that over the next 255 ms the amount of total spin remained unchanged and a new radical that was weakly exchange coupled to cob(II)alamins was generated. We now propose that this initially formed radical is **13** (Scheme 3) and that it partitions into two major pathways (Scheme 3A,B). Pathway A results in covalent modification of RTPR by the sugar moiety of F_2CTP and is the focus of this paper, while pathway B results in the production of 0.25−0.3 equiv of a stable cytidine nucleotide radical and is the focus of the preceding paper (*27*). These two pathways account for 0.75−0.8 equiv of F_2CTP consumed in the inactivation study, which is sufficient for complete RTPR inactivation, given that our previous pre-steady state experiments have indicated that only 75−80% of our recombinant protein is active (*47*, *53*−*55*).

Similarites of the Mechanism of Inactivation of RTPR by F_2CTP and Class Ia (E. coli and human with β2 or p53β2) RNRs by F_2CDP. First, in all RNRs that we have examined, inhibition by a gemcitabine nucleotide requires only a single nucleotide per α for complete inactivation (*24*, *25*). In class I RNRs that have complex quaternary structures ($\alpha_n\beta_m$, where n = 2, 4, or 6 and m = 2, 4, or 6), complete inactivation by one F_2CDP per α results from the increased affinity of the $\alpha_n\beta_m$ subunits because of the inactivation in one αβ pair. Second, despite the stoichiometry of the inhibition reaction, there are at least two pathways responsible for inactivation: one involving covalent modification and one involving destruction of the cofactor (pathways A and B, respectively, in Scheme 3). Third, there are ~0.5 label from the sugar moiety of [1′-^{3}H]F_2CTP that becomes covalently attached to α. The attachment site(s) is chemically labile, making identification of these sites challenging. Fourth, in all cases, the sugar-modified α subunit of RNR migrates on a SDS−PAGE gel as a protein with a higher molecular mass than the unmodified RNR. Fifth, all RNRs inactivated by F_2CD(T)Ps are accompanied by release of approximately one cytosine and the loss of two fluoride ions.

Scheme 3: Proposed Mechanism of Inactivation of RTPR by F_2CTP by the Nonalkylative and Alkylative Pathways

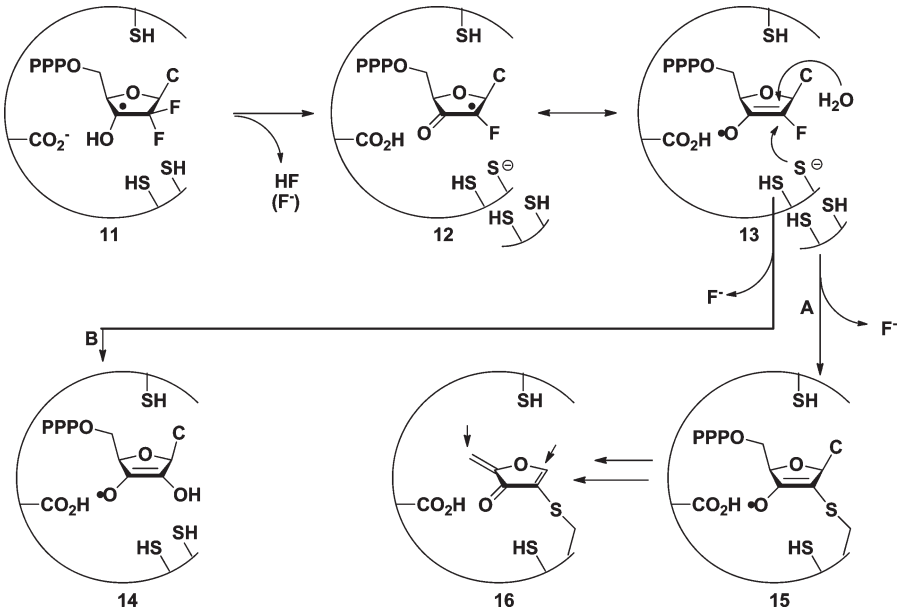

Scheme 4: Proposed Mechanism for Generation of Furanone during the Inactivation of RTPR with F_2CTP

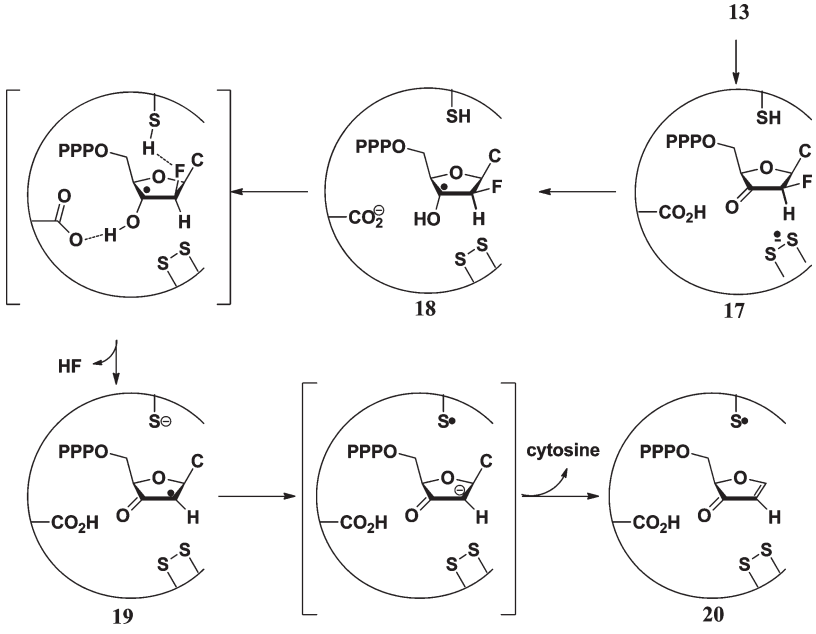

The data, in sum, suggest that the mechanism of inactivation of RNRs by Gemzar nucleotides does in fact follow the paradigm for other 2′-substituted nucleotide mechanism-based inhibitors (Scheme 1). The loss of the second fluoride ion, however, makes the mechanism of F_2CD(T)P more complex than the generic mechanism for the 2′-monosubstituted deoxynucleotide mechanism-based inhibitors (Scheme 1). However, we propose that the predominant mechanism of loss of the second fluoride is also likely to be similar in all RNRs (Scheme 3).

Proposed Mechanisms of Covalent Modification of RTPR. The mechanism of covalent labeling of RTPR is complex, and many possibilities have been considered. Our current model in Scheme 3 proposes that **13** is common in all pathways. Evidence in support of this intermediate comes from the trapping of 2′-deoxy-2′-fluorocytidine subsequent to the inactivation of C119S-RTPR with F_2CTP using $NaBH_4$. To account for the majority of labeled RTPR (pathway A of Scheme 3), C_{119} or C_{408} is proposed to directly attack C2′ of **13**. This attack would prevent escape of the sugar moiety from the active site and allow the trapped sugar to reside in the active site long enough to lose tripolyphosphate. Subsequent alkylation could then occur at C1′ or C5′ (**16**, Scheme 3), providing an explanation for our inability to isolate well-behaved peptide adducts (Figure 1). In the class Ia RNR inactivation studies, mutagenesis studies suggest that the C_{119} equivalent is involved in covalent labeling (*23*−*25*). In the case of RTPR, at most 30% of the covalent modification could arise from this cysteine. Additional labeling could potentially come from C_{408}. In pathway B, instead of attack by C_{119} or C_{408}, attack by an active site H_2O is proposed, leading to **14**. The evidence that supports this proposal is described in the preceding paper (*27*).

Our characterization of the radiolabeled C-terminal peptide of RNR suggests that covalent modification is more complex than that indicated in Scheme 3. A portion (10−15%) of the covalent

labeling requires an additional pathway as the mass spectrometric data suggest that F_2CTP is converted to a furanone (Scheme 2) that alkylates one or both of the C-terminal cysteines of RTPR. It is difficult to rationalize how these adducts could be generated from **15** (Scheme 3). A proposal for the generation of the furanone is shown in Scheme 4. This mechanism starts with common intermediate **13**. However, in this pathway, **13** is reduced by a mechanism similar to that proposed for CTP reduction, involving intermediates **17** and **18**. This intermediate can now lose HF to generate **19**, which subsequent to electron transfer from C_{408} would rapidly eliminate cytosine. Intermediate **20** can only be alkylated by the C-terminal cysteines as the active site cysteines involved in nucleotide reduction are in a disulfide. Once the first alkylation occurs, tripolyphosphate can eventually be released and the second alkylation can occur.

SUMMARY

The mechanism of F_2CTP inactivation of RTPR is complex even though it is stoichiometric. Perhaps most surprising is the fact that the remarkable number of similarities in the mechanism of inactivation shared between the class II RNR described in this work and the preceding paper (*27*) and the class I RNRs. Understanding the details of this simpler system may help to unravel class I RNRs, targets of this antitumor agent.

ACKNOWLEDGMENT

We thank Dr. Aaron Hoskins for thoughtful review of the manuscript and Dr. John Leszyk at UMass Medical School for performance and assistance with interpretation of the mass spectrometry experiments.

SUPPORTING INFORMATION AVAILABLE

Outline of F_2C synthesis (Scheme S1), depiction of PSD peptide fragments (Scheme S2), and MS/MS analysis of the 2020 Da RTPR peptide (Figure S1). This material is available free of charge via the Internet at http://pubs.acs.org.

REFERENCES

1. Matsuda, A., and Sasaki, T. (2004) Antitumor activity of sugar-modified cytosine nucleosides. *Cancer Sci. 95*, 105–111.
2. Plunkett, W., Huang, P., and Gandhi, V. (1997) Gemcitabine: Actions and interactions. *Nucleosides Nucleotides 16*, 1261–1270.
3. Plunkett, W., Huang, P., Xu, Y.-Z., Heinemann, V., Grunewald, R., and Gandhi, V. (1995) Gemcitabine: Metabolism, mechanisms of action, and self-potentiation. *Semin. Oncol. 2*, 3–10.
4. Rivera, F., López-Tarruella, S., Vega-Villegas, M. E., and Salcedo, M. (2009) Treatment of advanced pancreatic cancer: From gemcitabine single agent to combinations and targeted therapy. *Cancer Treat. Rev. 35*, 335–339.
5. Danesi, R., Altavilla, G., Giovannetti, E., and Rosell, R. (2009) Pharmacogenetics of gemcitabine in non-small-cell lung cancer and other solid tumors. *Pharmacogenetics 10*, 69–80.
6. Hui, Y. F., and Reitz, J. (1997) Gemcitabine: A cytidine analogue active against solid tumors. *Am. J. Health-Syst. Pharm. 54*, 162–170.
7. Cersosimo, R. J. (2002) Lung cancer: A review. *Am. J. Health-Syst. Pharm. 59*, 611–642.
8. Lidestahl, A. (2006) Efficacy of systemic therapy in advance pancreatic carcinoma. *Acta Oncol. 45*, 136–143.
9. Rosti, G. (2006) Small cell lung cancer. *Ann. Oncol. 17*, 5–10.
10. Oettle, H., Arnold, D., Hempel, C., and Riess, H. (2000) The role of gemcitabine alone and in combination in the treatment of pancreatic cancer. *Anti-Cancer Drugs 11*, 771–786.
11. Nabhan, C., Krett, N., Gandhi, V., and Rosen, S. (2001) Gemcitabine in hematologic malignancies. *Curr. Opin. Oncol. 13*, 514–521.
12. Colomer, R. (2005) Gemcitabine plus taxane combination in metastatic breast cancer: A comprehensive review. *EJC Suppl. 3*, 9–16.
13. Akerele, C. E., Rybalova, I., Kaufman, H. L., and Mani, S. (2003) Current approaches to novel therapeutics in pancreatic cancer. *Invest. New Drugs 21*, 113–129.
14. Schrader, A. J., Varga, Z., Hegele, A., Pfoertner, S., Olbert, P., and Hofmann, R. (2006) Second-line strategies for metastatic renal cell carcinoma: Classics and novel approaches. *J. Cancer Res. Clin. Oncol. 132*, 137–149.
15. Barlési, F., and Pujola, J.-L. (2005) Combination of chemotherapy without platinum compounds in the treatment of advanced non-small cell lung cancer: A systematic review of phase III trials. *Lung Cancer 49*, 289–298.
16. Rosenberg, J. E., Carroll, P. R., and Small, E. J. (2005) Update on chemotherapy for advanced bladder cancer. *J. Urol. 174*, 14–20.
17. Pauwels, B., Korst, A. E. C., Lardon, F., and Vermorken, J. B. (2005) Combined modality therapy of gemcitabine and radiation. *Oncologist 10*, 34–51.
18. Heinemann, V., Xu, Y.-Z., Chubb, S., Sen, A., Hertel, L. W., Grindey, G. B., and Plunkett, W. (1990) Inhibition of ribonucleotide reduction in CCRF-CEM cells by 2′,2′-difluorodeoxycytidine. *Mol. Pharmacol. 38*, 567–572.
19. Baker, C. H., Banzon, J., Bollinger, J. M., Jr., Stubbe, J., Samano, V., Robins, M. J., Lippert, B., Jarvi, E., and Resvick, R. (1991) 2′-Deoxy-2′-methylenecytidine and 2′-deoxy-2′,2′-difluorocytidine 5′-diphosphates: Potent mechanism-based inhibitors of ribonucleotide reductase. *J. Med. Chem. 34*, 1879–1884.
20. van der Donk, W. A., Yu, G., Pérez, L., Sanchez, R. J., and Stubbe, J. (1998) Detection of a new substrate-derived radical during inactivation of ribonucleotide reductase from *Escherichia coli* by gemcitabine 5′-diphosphate. *Biochemistry 37*, 6419–6426.
21. Silva, D. J., Stubbe, J., Samano, V., and Robins, M. J. (1998) Gemcitabine 5′-triphosphate is a stoichiometric mechanism-based inhibitor of *Lactobacillus leichmannii* ribonucleoside triphosphate reductase: Evidence for thiyl radical-mediated nucleotide radical formation. *Biochemistry 37*, 5528–5535.
22. Licht, S., and Stubbe, J. (1999) Mechanistic investigations of ribonucleotide reductases. In Comprehensive Natural Products Chemistry (Barton, S. D., Nakanishi, K., Meth-Cohn, O., and Poulter, C. D., Eds.) pp 163−203, Elsevier Science, New York.
23. Wang, J., Lohman, G. J., and Stubbe, J. (2007) Enhanced subunit interactions with gemcitabine-5′-diphosphate inhibit ribonucloetide reductases. *Proc. Natl. Acad. Sci. U.S.A. 104*, 14324–14329.
24. Wang, J., Lohman, G. J., and Stubbe, J. (2009) Mechanism of inactivation of human ribonucleotide reductase with p53R2 by gemcitabine-5′-diphosphate. *Biochemistry 48*, 11612–11621.
25. Artin, E., Wang, J., Lohman, G. J. S., Yu, G., Griffin, R. G., Barr, G., and Stubbe, J. (2009) Insight into the mechanism of inactivation of ribonucleotide reductase by gemcitabine 5′-diphosphate in the presence and absence of reductant. *Biochemistry 48*, 11622–11629.
26. Cerqueira, N. M. F. S. A., Fernandes, P. A., and Ramos, M. J. (2006) Enzyme ribonucleotide reductase: Unraveling an enigmatic paradigm of enzyme inhibition by furanone derivatives. *J. Phys. Chem. B 110*, 21272–21281.
27. Lohman, G. J. S., and Stubbe, J. (2010) Inactivation of *Lactobacillus leichmannii* ribonucleotide reductase by F_2CTP: adenosylcobalamin destruction and formation of a nucleotide based radical. *Biochemistry 49*, DOI: 10.1021/bi9021318.
28. Usova, E. V., and Eriksson, S. (1997) The effects of high salt concentrations on the regulation of the substrate specificity of human recombinant deoxycytidine kinase. *Eur. J. Biochem. 248*, 762–766.
29. van Rompay, A. R., Johansson, M., and Karlsson, A. (1999) Phosphorylation of deoxycytidine analog monophosphates by UMP-CMP kinase: Molecular characterization of the human enzyme. *Mol. Pharmacol. 56*, 562–569.
30. Artin, E. (2006) Mechanistic studies of the Class I ribonucleotide reductase from *Escherichia coli*. Thesis in Chemistry, Massachusetts Institute of Technology, Cambridge, MA.
31. Lunn, C. A., Kathju, S., Wallace, B. J., Kushnern, S. R., and Pigiet, V. (1984) Amplification and purification of plasmid-encoded thioredoxin from *Escherichia coli* K12. *J. Biol. Chem. 259*, 10469–10474.
32. Russel, M., and Model, P. (1985) Direct cloning of the trxB gene that encodes thioredoxin reductase. *J. Bacteriol. 163*, 238–242.
33. Booker, S., and Stubbe, J. (1993) Cloning, sequencing and expression of the adenosylcobalamin-dependent ribonucleotide reductase from *Lactobacillus leichmannii. Proc. Natl. Acad. Sci. U.S.A. 90*, 8352–8356.
34. Chou, T. S., Heath, P. C., Patterson, L. E., Poteet, L. M., Lakin, R. E., and Hunt, A. H. (1992) Stereospecific synthesis of 2-deoxy-2,2-difluororibonolactone and its use in the preparation of 2′-deoxy-2′,2′-difluoro-β-D-ribofuranosyl pyrimidine nucleosides: The key role of selective crystallization. *Synthesis* 565–570.

35. Dawson, R. M. C., Elliot, D. C., Elliot, W. H., and Jones, K. M. (1986) Data for biochemical research, 3rd ed., Clarendon Press, Oxford, U.K.
36. Kohn, P., Samaritano, R. H., and Lerner, L. M. (1965) A new method for the synthesis of furanose derivatives of aldohexoses. *J. Am. Chem. Soc. 87*, 5475–5480.
37. Brown, H. C. (1975) in Organic Synthesis via Boranes, pp 18−21, 29−31, 51−55, John Wiley and Sons, New York.
38. Brown, H. C., and Tierney, P. A. (1958) The reaction of lewis acids of boron with sodium hydride and borohydride. *J. Am. Chem. Soc. 80*, 1552–1558.
39. Examples of this procedure: Kaulinya, L. T., and Lidak, M. Y. (1987) *Chem. Heterocycl. Compd. 23*, 77–81. Novikov, M. S., Ozerov, A. A., Brel, A. K., Boreko, E. I., Korobchenko, L. V., and Vladyko, G. V. (1994) *Pharm. Chem. J. 28*, 110–113.
40. Garrett, C., and Santi, D. V. (1979) Rapid and sensitive high-pressure liquid-chromatography assay for deoxyribonucleoside triphosphates in cell-extracts. *Anal. Biochem. 99*, 268–273.
41. Steeper, J. R., and Steuart, C. C. (1970) A rapid assay for CDP reductase activity in mammalian cell extracts. *Anal. Biochem. 34*, 123–130.
42. Mass spectrometry described herein and the fragment analysis were performed by Dr. John Leszyk (UMass Medical School, Proteomic Mass Spectrometry Lab, Shrewsbury, MA).
43. Data processing was performed using Kompact version 2.2.1 (Kratos Analytical Ltd., Manchester, U.K.). Fragment searching and analysis was performed by Dr. John Leszyk using Mascot, Matrix Science Ltd., Boston, MA.
44. Ireton, G. C., McDermott, G., Black, M. E., and Stoddard, B. L. (2002) The structure of *Escherichia coli* cytosine deaminase. *J. Mol. Biol. 315*, 687–697.
45. Lohman, G. J. S. (2006) Thesis in Chemistry, Massachusetts Institute of Technology, Cambridge, MA.
46. Ashley, G. W., Harris, G., and Stubbe, J. (1988) Inactivation of the *Lactobacillus leichmannii* ribonucleoside triphosphate reductase by 2′-chloro-2′-deoxyuridine 5′-triphosphate: Stoichiometry of inactivation, site of inactivation, and mechanism of the protein chromophore formation. *Biochemistry 27*, 4305–4310.
47. Booker, S., Licht, S., Broderick, J., and Stubbe, J. (1994) Coenzyme B_{12}-dependent ribonucleotide reductase: Evidence for the participation of five cysteine residues in ribonucleotide reduction. *Biochemistry 33*, 12676–12685.
48. Mao, S. S., Holler, T. P., Yu, G. X., Bollinger, J. M., Jr., Booker, S., Johnston, M. I., and Stubbe, J. (1992) A model for the role of multiple cysteine residues involved in ribonucleotide reduction: Amazing and still confusing. *Biochemistry 31*, 9733–9743.
49. Åberg, A., Hahne, S., Karlsson, M., Larsson, Å., Ormö, M., Åhgren, A., and Sjöberg, B.-M. (1989) Evidence for two different classes of redox-active cysteines in ribonucleotide reductase of *Escherichia coli*. *J. Biol. Chem. 264*, 12249–12252.
50. Lin, A.-N. I., Ashley, G. W., and Stubbe, J. (1987) Location of the redox-active thiols of ribonucleotide reductase: Sequence similarity between the *Escherichia coli* and *Lactobacillus leichmannii* enzymes. *Biochemistry 26*, 6905–6909.
51. Ashcroft, A. E. An Introduction to Mass Spectrometry http://www.astbury.leeds.ac.uk/facil/MStut/mstutorial.htm.
52. Dass, C. (2004) An Introduction to Biological Mass Spectrometry, John Wiley & Sons, New York.
53. Licht, S. S., Booker, S., and Stubbe, J. (1999) Studies on the catalysis of carbon-cobalt bond homolysis by ribonucleoside triphosphate reductase: Evidence for concerted carbon-cobalt bond homolysis and thiyl radical formation. *Biochemistry 38*, 1221–1233.
54. Licht, S. S., Lawrence, C. C., and Stubbe, J. (1999) Thermodynamic and kinetic studies on carbon-cobalt bond homolysis by ribonucleoside triphosphate reductase: The importance of entropy in catalysis. *Biochemistry 38*, 1234–1242.
55. Licht, S. S., Lawrence, C. C., and Stubbe, J. (1999) Class II ribonucleotide reductases catalyze carbon-cobalt bond reformation on every turnover. *J. Am. Chem. Soc. 121*, 7463–7468.